Thermal and radiation-enhanced diffusion in Cu_3Au

Y. S. Lee and C. P. Flynn
Department of Physics, University of Illinois at Urbana-Champaign, Urbana, Illinois 61801

R. S. Averback
Department of Materials Science and Engineering, University of Illinois at Urbana-Champaign, Urbana, Illinois 61801

(Received 12 October 1998)

Thermal and radiation-enhanced diffusion in thin films of the order-disorder alloy Cu_3Au have been analyzed above and below the transition temperature. It is demonstrated that thin films grown by molecular beam epitaxy are uniquely suited for such experiments as the surface provides a dominant and well-characterized sink for migrating defects. The analysis is applied to recent experiments. Quantitative predictions of radiation-enhanced diffusion agree closely with experimental values. Analysis of the tracer-impurity thermal diffusion experiments provide host diffusion coefficients in a temperature regime through the transition temperature which were heretofore unavailable. [S0163-1829(99)13725-1]

I. INTRODUCTION

Irradiation of solids with energetic particles leads to the displacement of atoms from their lattice sites through energetic recoil processes. Most displaced atoms quickly relocate back onto nearby vacated lattice sites, but a small fraction remain as interstitials, with a compensating number of unfilled vacancies left behind. Since the characteristic energy for displacements far exceeds kT_m (T_m is the melting temperature) atomic relocations occur in absence of significant influences from thermodynamic forces in most systems, evoking the descriptive term ballistic mixing. In ordered phases and compounds, ballistic mixing results in chemical disorder, and in some cases amorphization as well. At elevated temperatures, point defects are mobile and therefore diffusional processes are enhanced by irradiation. Thermally activated diffusive processes tend to restore a system to its equilibrium state.

While experiments and computer simulations have now provided a firm background for understanding the defect production process during irradiation of crystalline solids,[1] predicting the microstructural development of irradiated alloys during prolonged irradiation at elevated temperatures remains a difficult problem and largely unsolved. Much of the reason for this is that many kinetic pathways are opened by the energetic displacement process and they are separated by only small energy differences. In attempts to clarify the kinetic behavior of irradiated alloys, it has long been realized that irradiation studies on order-disorder alloys are especially illuminating.[2] Following these past studies, we have begun a series of irradiation experiments on these systems, but with the added feature that we employ highly perfect thin-film specimens. As we will show, our ability to control the sink structure for migrating defects through the film thickness greatly enhances the information that can be drawn from these experiments. In the present study, we investigate thermal and radiation-enhanced diffusion in Cu_3Au both above and below the critical temperature for ordering, T_c, and thereby clarify the effects of order on these diffusion processes. The experimental data presented here have been reported previously;[3] the primary purpose of the present paper is to provide a thorough analysis of these data and to illustrate the potential of thin-film experiments for future investigations.

II. EXPERIMENTAL PROCEDURES

The experimental procedures employed in obtaining the various diffusion coefficients are described elsewhere,[3] and we simply state here those features necessary for comprehending the analysis that follows.

(i) The measurements were of tracer impurity diffusion, Ni and Pd, in Cu_3Au. Ni resides on the Cu sublattice and Pd on the Au sublattice.

(ii) The samples were grown by molecular-beam epitaxy (MBE) methods. They consisted of ≈300 nm thick layers of Cu_3Au grown epitaxially in the (111) orientation on Nb(110). Thin tracer layers (≈4 nm) of either Cu_6AuPd on Cu_2NiAu were introduced at the midplanes of the Cu_3Au films.

(iii) The composition of the films were within ≈1% of correct stoichiometry.

(iv) The radiation-enhanced diffusion coefficient refers to the total diffusion coefficient under irradiation less the contributions from thermal diffusion and ion beam mixing.

(v) The ion doses are provided in units of displacements per atom (dpa) which were determined using TRIM91 (Ref. 4) for simulation. The displacement rate for the He irradiation, ($\mathrm{dpa\,s^{-1}}$) was calculated to be 7.6×10^{-5} using an assumed displacement energy of 25 eV. The total ion fluence employed in these experiments was $2\times10^{17}\,\mathrm{cm^{-2}}$, which corresponds to 0.2 dpa.

III. EXPERIMENTAL RESULTS

A. Thermal diffusion coefficients

Thermal diffusion coefficients for Ni and Pd in Cu_3Au are shown in Fig. 1 in an Arrhenius plot of D against T^{-1}, along with other data to be discussed in Sec. IV. The significant features of these data are as follows. Above the ordering

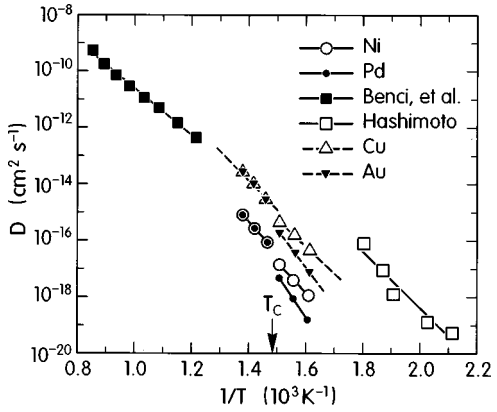

FIG. 1. Thermal diffusion coefficients from Ref. 5 (filled squares), Ref. 6 (open squares), and the present tracer impurity diffusion coefficients (open and filled circles connected by solid lines). Predicted host diffusion coefficients are indicated by open and filled triangles connected by dashed lines.

temperature the diffusion coefficients for Ni and Pd, D_{Ni} and D_{Pd}, have the same value to within the experimental uncertainties, ≈30%. The activation enthalpy for diffusion in this regime is 2.3 ± 0.3 eV. Below the transition temperature D_{Ni} is larger than D_{Pd}, with respective activation enthalpies of 2.15 ± 0.3 eV and 2.9 ± 0.4 eV. Also noteworthy is that as the temperature is lowered through the transition temperature, D_{Ni} and D_{Pd}, appear to drop discontinuously, by a factor of ≈2.3 for Ni and a factor of ≈4.5 for Pd.

B. Radiation-enhanced diffusion

The results for the radiation-enhanced diffusion coefficients, $D_{\mathrm{Ni}}^{\mathrm{RED}}$ and $D_{\mathrm{Pd}}^{\mathrm{RED}}$, are illustrated in Fig. 2 for both Ni and Pd. These data were obtained, as described in Ref. 3, by subtracting the contribution of ion beam mixing from the measured mixing profiles. This was done since ion beam mixing arises from the defect production process and is distinct from diffusion mediated by the motion of radiation-induced point defects. The RED behavior mirrors the thermal diffusion behavior in several ways: $D_{\mathrm{Ni}}^{\mathrm{RED}}$ and $D_{\mathrm{Pd}}^{\mathrm{RED}}$ have

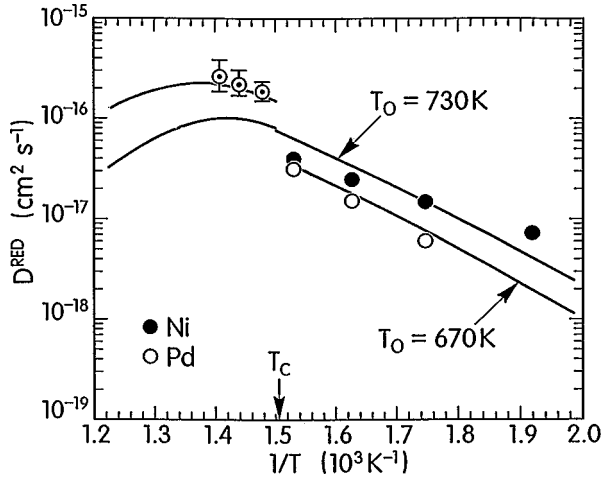

FIG. 2. Radiation enhanced diffusion coefficients of Ni and Pd in Cu_3Au during 1.0 MeV He irradiation. Also shown are predictions for enhanced diffusion coefficients of Ni using Eq. (7).

equal values above the transition temperature; they then drop abruptly on ordering at T_c, in this case by a factor of ≈4.6 for both Ni and Pd; and finally they diverge as the temperature is lowered below T_c. The apparent activation energies in the low temperature regime are 0.38 ± 0.06 and 0.62 ± 0.09 eV for Ni and Pd, respectively.

It may be noted that the error bars assigned to the data are greater above T_c than below it. This asymmetry arises from the increasingly larger fraction of the thermal contribution to the total diffusion coefficient. At $1000/T = 1.4$, for example, equilibrium thermal diffusion is more than twice radiation-enhanced diffusion. Owing to this experimental difficulty, we disregard the slope in these data above T_c and rely only upon the magnitude of the data in this regime for our interpretation. Below T_c, the thermal contribution is less than ≈20%.

IV. DISCUSSION

A. Thermal diffusion in Cu_3Au

In Sec. III A we summarized measurements of Ni and Pd impurity diffusion in Cu_3Au. Earlier research has examined Au tracer diffusion above the ordering temperature, and an average of Cu and Au diffusion below T_c. Our purpose here is first to compare the present results with the earlier work in order to understand the relationship between the impurity and host diffusion, and second, to discuss the significance of the present observations with regard to the effect of ordering on the diffusion process.

Figure 1 shows in addition to our own impurity diffusion data, represented by open and filled circles, two other available sets of data for diffusion in Cu_3Au. Filled squares represent the results of Au tracer measurements by Benci *et al.*[5] through the temperature range extending from near the liquidus down to ≈500 °C, or about 155 °C above T_c. Open squares at low temperature, below T_c, represent diffusion rates inferred by Hashimoto and Yamomoto from observations of vacancy evaporation from voids.[6] In brief summary of these collected results we note first that the two sets of host diffusion data are in rough agreement in overall trend, although the activation energies the authors quote from the separate apparent slopes of their data sets differ widely. Second, the present results for impurity diffusion lie markedly below the joint trend of the host diffusion results. In what follows, the discussion focuses initially on this difference between the reported host and the current impurity diffusion rates.

Differences between host and impurity diffusion in metals have been recognized for five or more decades and have been treated by semiquantitative theories.[7] There are two main effects. Both impurities and vacancies disturb the perfect metal and, when in close proximity, these two defects experience an interaction that modifies their energy and hence the probability with which the vacancy is found as a neighbor of the impurity. This affects the impurity diffusion rate directly, and also through the fact that binding causes the two to linger together and increases the probability of immediate return jumps. A further effect is that the impurity has vibrational structure that differs from that of the host, and both the frequency factors and migration energies may thereby differ. As a result of these several processes, it is commonplace for

impurities in metals to differ from host species by small increments in both the activation energy and the frequency factor.

For the cases of Ni and Pd interacting with Cu and Au, a body of information is available.[8] We now employ these results to improve the understanding of the diffusion data in Fig. 1. Ni impurities are observed to diffuse a factor of about 27 times slower than host Cu atoms in pure Cu near 395 °C, while, in extrapolated results, Pd atoms at 395 °C diffuse about 50 times slower than host Au in pure Au. In both cases the activation energy of the impurity exceeds that of the host by about 0.26 eV. Both cases conform well to a geometrical average:

$$\frac{D_h}{D_i} = 37 e^{(0.26\ \mathrm{eV}/k)(T^{-1}-T_c^{-1})}, \tag{1}$$

where D_h and D_i refer to host and impurity diffusion, respectively. In contrast Au diffusion never differs by as much as a factor 2 from host Cu over the entire temperature range down from the melting point to 395 °C, and the same holds in the extrapolated results for Cu in Au. Our own results similarly show closely equal diffusion rates for Ni and Pd above the ordering temperature in Cu_3Au.

The strongly systematic chemical character of these results is further confirmed when Eq. (2) is now employed for Cu_3Au to predict host diffusion rates through T_c (which remain unknown) from the present Ni and Pd impurity results. These predictions are shown by open and closed triangle symbols connected by a broken line in Fig. 1. Above the transition the diffusion coefficients, with corrections for impurity effects estimated in this way, agree quite well with the trend of the actual measurements of Benci *et al.* The abrupt changes remain at the ordering transition, and the diffusion below T_c reproduces much as before but with smaller slopes. In the absence of direct measurements we believe that the corrected impurity rates in Fig. 1 provide the best present estimates of the Cu and Au diffusion through the region of the transition.

The corrected diffusion data maintain the discontinuities of the impurity results at T_c, which means that the estimated Cu diffusion decreases by a factor 2 at the transition while that of Au decreases by a factor 5. The different behaviors of the two tracers is convincing proof that they reside mainly on separate sublattices, as intended. In interpreting the observation for Cu we note that Ito *et al.* give the correlation factor for vacancy diffusion on the Cu sublattice of Cu_3Au as 0.689 as compared to the fcc value of 0.781.[9] In addition, however, the ordering decreases the number of nearest neighboring Cu sites from 12 to 8, decreasing the number of jump paths by a factor 3/2. In all, the diffusion rate in the fully ordered structure is thus decreased by a factor $8\times0.689/12\times0.781 = 0.59$, which is reasonably consistent with the observed factor 0.5.

A comparable treatment of Au would predict that its diffusion is entirely suppressed below T_c since, in the ordered structure, no Au first neighbors remain through which Au diffusion can proceed. Huntington showed that the interchange of two Au atoms in fully ordered Cu_3Au atoms requires at least six vacancy jumps, with transient Cu occupancy of both Au sites, and with Au passing through intermediate Cu sites.[10] Mechanisms of this type have been discussed by several researchers.[11–13] Not only are the paths complicated but energetic factors from the necessary antisite occupancy also inhibit Au diffusion in a way not present for Cu diffusion. Indeed, the Au effective activation energy of 2.9 eV below T_c is larger than the value 1.9 eV for Cu (values corrected for impurity effects) for precisely this reason. It might be thought that this impediment to diffusion could cause a much stronger suppression on the Au sublattice than the factor 5 actually observed. The explanation is that the lattice is not in fact fully ordered but that Au occupies Cu sites with a probability that is estimated from x-ray measurements at about 20% at T_c (Ref. 14) and with considerably larger estimates still from resistance measurements.[15] Since the Au diffusion rate is only 40% of the Cu rate, this means that half or more of the Au diffusion in the ordered phase near T_c can be identified directly with Au atoms jumping among Cu sites. A more detailed analysis is hampered by uncertainty in the degree of equilibrium order. It is nevertheless clear that the discontinuities in diffusion that take place at T_c compare well in general magnitude with the expectations of simple models related to the jump paths and site occupation probabilities that describe the ordered phase.

An interesting perspective on the increased Au activation energy below T_c is obtained by comparison with the case of $RbAg_4I_5$. In this material an order-disorder transformation occurs by a divergence in Frenkel pair formation, in effect liquefying the Ag sublattice above its critical temperature, with a phase transition which is closely of second order. This is a fortunate example in that the diffusion coefficient can be determined simply and accurately from the electrical conductivity. Combined resistance and heat capacity measurements revealed that the activation energy for diffusion contained the ordering energy of the lattice, which related the diffusion anomaly to the specific heat anomaly in a quantitative way.[16] The present example of Cu_3Au is less convenient because the diffusion can be measured only in a small temperature range near T_c, and then only with some effort. Nevertheless, the larger activation energy for Au diffusion must in part reflect the ordering energy, in analogy with the case of $RbAg_4I_5$. The fact that the Cu_3Au lattice undergoes such a small fractional disordering below T_c presumably reduces the extent to which the degree of order modifies the energetics of the observed diffusion, and the discontinuity at T_c measures the main effect.

B. Radiation-enhanced diffusion in Cu_3Au

We turn now to an interpretation of the results presented in Sec. III B for radiation enhanced diffusion caused by 1.0 MeV He irradiation of Cu_3Au. A convenient feature of the present work is that we can identify with some confidence the regime of enhanced diffusion produced by the present level of ion beam flux. Specifically, at the highest temperatures employed here, the ion flux is only just sufficient to enhance the diffusion by a small factor of order unity. This evidence that the excess defect populations added by irradiation at $T\sim730$ K are modest in fractional size proves sufficient, given the remaining results, to provide a comprehensive overview of the effect of irradiation on the defect populations. It is to a discussion of this matter that we turn first.

The effect of an ion beam in creating point defects in any given material in now quite well understood;[1,17] it is the further complications from mobility and defect reactions that remain still to be unraveled in most instances. As noted previously, the calculated displacement rate for the 1 MeV He irradiations in these experiments was 7.6×10^{-5} dpa s^{-1}. Past experimental work[18] and recent molecular dynamics simulations[1,17] have shown that under the irradiation conditions employed here, the Kinchin-Pease expression overestimates the true defect production by a factor of $\approx$2.5. The resulting displacement rate is reduced another factor of about two owing to immediate recombination of close Frenkel pairs.[1] The net formation rate of defects that contribute to the diffusion process is thus $\approx$20% of the Kinchin-Pease value, or $\approx1.5\times10^{-5}$ Frenkel pairs per atom in the current situation. The state of understanding is such that the estimate can be relied on to within a factor of 2.

The analysis of the results that follows turns on a single physical point which is of critical importance. Specifically, the defect production rate calculated above, for the flux employed in the experiments, is so small that our observation of radiation enhanced diffusion at temperatures above the ordering temperature can result only from particular, well-defined conditions of the defect system that exists in the irradiated sample. The degree to which irradiation causes defect populations to be enhanced depends on the distances defects must subsequently diffuse before annihilating: the longer the required diffusion path the greater the resulting concentration increase caused by a given level of irradiation. What we now show is that the defect enhancement just above T_c, signaled by the observed enhanced diffusion, is uniquely consistent with diffusion lengths corresponding to the most remote known sinks. These are the sites of defect sinks offered by the front surface of the sample. If closer fixed sinks existed in the bulk of the sample, or if a significant fraction of the defects decayed by recombination, then the diffusion path would be reduced and the concentration reduced such that it would no longer be possible to interpret the observed radiation enhancement of the diffusion.

The principle of this demonstration is conveyed in simplified form by considering a uniform concentration c of defects that drain by diffusion to sinks with time constant τ according to the equation

$$dc/dt = K - (c-\overline{c})/\tau. \tag{2}$$

Here K is the creation rate due to the radiation field and $\overline{c}/\tau$ the thermal creation rate from fixed sinks required to obtain the thermal equilibrium concentration $c=\overline{c}$ for $K=0$. The steady state solution (for $dc/dt=0$) with $K\neq0$ is

$$c-\overline{c}=K\tau. \tag{3}$$

This shows that the largest possible enhancement occurs for the largest possible value of the time constant τ, as stated above. Smaller values of τ which might result, for example, from closer sinks, or added losses from recombination, would both increase the loss rate and decrease the enhanced defect population.

We now show that the observed enhancement corresponds to diffusion of point defects all the way to the free epilayer surface; any shorter diffusion path would suppress the irradiation-induced defect population in contradiction with the observations. Diffusion to fixed sinks is treated by an expansion in orthogonal eigenfunctions of the diffusion equation, $c_i(\mathbf{r},t)=c_i(\mathbf{r})\exp-t/\tau_i$, in which the spatial factors have mean square displacements from the sinks that satisfy $\langle r^2\rangle_i\sim D\tau_i$. In an Appendix it is shown for vacancy diffusion from an epilayer of thickness L to the single free surface that the longest time constant, which describes most of the annealing, is given by

$$\tau^{-1}=\kappa_0^2 D_v, \quad \kappa_0^2=(\pi/2L)^2. \tag{4}$$

Hence the defect loss rate $\overline{c}/\tau$ per site in thermal equilibrium is $\kappa_0^2 D_v\overline{c}=\kappa_0^2 D/f_v$, in which D is the ionic diffusion coefficient and $f_v=0.781$ is the correlation factor for ionic diffusion by the vacancy mechanism in the fcc lattice. In Fig. 3 we show $\kappa_0^2 D_{\mathrm{Cu}}/f_v$ as a function of T^{-1} using the measured host D_{Cu}, as estimated in Fig. 1, and the value $\kappa_0^2=2.74\times10^{13}\,\mathrm{m}^{-2}$ corresponding to a 300 nm film. Also shown as a broken line in the figure is the value $K_0=1.5\times10^{-5}\,\mathrm{s}^{-1}$ cited above for the vacancy creation rate by irradiation. The loss rate crosses the creation rate at $T\approx700$ K or just above the ordering temperature. This is neatly consistent with the fact that radiation enhanced diffusion is indeed observed above the transition, which of course requires that a significant fractional increase of vacancy concentration be caused by the irradiation-induced defects, and which is possible only when the creation rate is comparable with or greater than the equilibrium loss rate to fixed sinks. Any larger equilibrium loss rate caused, for example, by closer sinks or paths reduced by recombination, would reduce the fractional change of diffusion attributable to irradiation. Notice conversely, that the nearly equal values of radiation enhanced and thermal diffusion coefficients at 700 K lend support to the accuracy of our values of K_0 and κ_0. To illustrate this point further we note that even a reduction of film thickness from 300 nm to 100 nm would increase κ_0^2 by a factor 9 and make any enhancement extremely difficult to observe above T_c, in contradiction with observation.

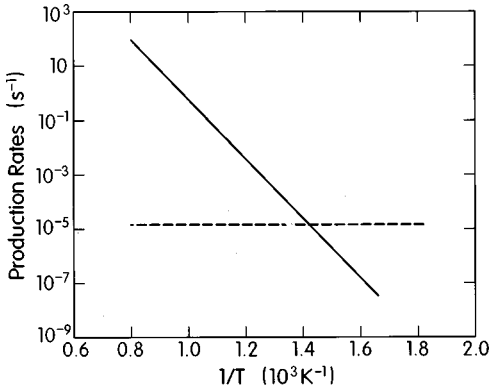

FIG. 3. Temperature dependence of the production of thermal vacancies. The temperature at which this rate equals the generation rate induced by ion irradiation, 1.5×10^{-5}, is indicated by the intersection of the two lines.

To progress further it is convenient to examine the order of the kinetics that determines the defect behavior under these experimental conditions. A typical defect requires about 5×10^5 steps in its random walk from the bulk to

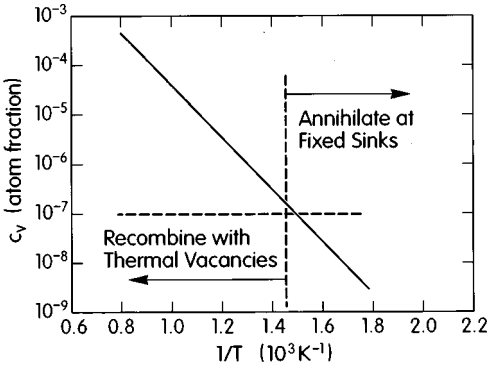

FIG. 4. Temperature dependence of the equilibrium concentration of vacancies. The horizontal line represents the equivalent number of vacancies required to present an equivalent sink strength for interstitials at the surface.

its annihilation at the front surface of a 300 nm film. If it inspects ~ 10 new sites each jump, any specific migrating defect needs a concentration $\sim 2\times 10^{-7}$ of opposite defects to offer equal chances of pair recombination and annihilation at the surface. In the Appendix it is shown that in the present instance of dominant vacancy disorder, the transition from first order to second order kinetics takes place when c_v increases to a level determined by a parameter x [see Eqs. (A17) and (A18) in the Appendix]. The numerator of x is the interstitial loss rate to recombination, and the denominator is the interstitial loss rate to fixed sinks, both evaluated for thermal equilibrium defect concentrations. Thus x measures the fraction of interstitials that recombine under conditions of weak or zero irradiation. Recombination must dominate for second order kinetics to prevail.

To find x we need the equilibrium vacancy concentration $\overline{c_v}$. An estimate can be made on the basis of general knowledge as

$$\overline{c_v}(T) = 7 \exp[-12000/T(\mathrm{K})]. \tag{5}$$

This employs a typical formation entropy factor $\sim 2k_B$ as the prefactor and an activation energy scaled to those of Cu and Au, so that the concentration is a typical value of about 3×10^{-4} at the melting point. The specific prediction for $T = 700\,\mathrm{K}$ (just above T_c) is a thermal vacancy concentration $\overline{c_v} = 2.5\times 10^{-7}$, which is probably correct to within an order of magnitude. Measurements on the mobility of vacancies in Cu_3Au along with the present thermal diffusion measurements, indicate, in fact, that this estimate is correct to within a factor of ≈ 3.[19] The value of $\overline{c_v}$ is shown at a function of T in Fig. 4. By means of a broken horizontal line the effective concentration of competing fixed sinks is also shown in Fig. 4 as obtained from the sample thickness L together with an estimate that the interstitial encounters 10 possible vacancy sites for recombination each jump. The intersection of these lines permits the identification, in the figure, first of the high temperature regime in which interstitials produced under very weak irradiation recombine, on average, with thermal vacancies, and second the low temperature regime in which the interstitials instead annihilate on average at fixed sinks. The crossover from one regime to the other occurs in the region near T_c (≈ 685 K); the figure indicates that, just above T_c, the interstitials created by weak irradiation of Cu_3Au have equal chances of reaching the surface or recombining with equilibrium vacancies. Since the radiation-enhanced and thermal diffusion coefficients in the experiments analyzed here are equal at ≈ 700 K, interstitials have nearly equal probabilities at this temperature of recombining with thermal vacancies or radiation-induced vacancies, or annihilating at sinks. At higher temperatures, they recombine with thermal vacancies and at lower temperatures they recombine with radiation-induced vacancies.

By these several arguments we are thus led to conclude first that the kinetics become linear just above T_c for the irradiation field employed in this research and, second, that at ≈ 700 K, the migration to free surfaces represents the characteristic diffusion length for annihilation of vacancies and interstitials.

Given these conclusions from semiquantitative arguments, let us now *assume* that the free surface alone is the dominant sink at ≈ 700 K, and that the kinetics indeed remain first order above this temperature. Equation (A21) now gives a quantitative prediction of the radiation-enhanced diffusion above T_c [see Eq. (A21) in the Appendix]. When evaluated this gives $2.2\times 10^{-15}\,\mathrm{cm^2/s}$ if $f_i = 0$ and $3.5\times 10^{-15}\,\mathrm{cm^2/s}$ if $f_i = 0.5$. This prediction is to be compared with the observed value of D_{RED} from Fig. 2 of about $6\times 10^{-15}\,\mathrm{cm^2/s}$ (when the value of $2\times 10^{-16}\,\mathrm{cm^2/s}$ for the tracers is increased by the factor of 37 from Sec. IV A to obtain equivalent values for the host species). This degree of agreement between the observed enhanced diffusion and a prediction derived solely from the sample thickness and the irradiation rate is, of course, very satisfactory, and adds to the confidence warranted by the interpretation.

The prediction of the radiation-enhanced diffusion establishes that at ≈ 700 K diffusion to the front surface of the sample represents the path length for vacancies to annihilate in the MBE grown thin films employed in the present research. This is an important result and of central interest for the design of future experimental studies of irradiation-induced defects using thin film samples. For example, under irradiation conditions where vacancies annihilate at the specimen surface, as in the present case just above T_c, the measured diffusion coefficients yield directly the absolute production rate of freely migrating defects, which was noted above. We also point out that the quality of materials produced by molecular beam epitaxy must be judged satisfactory in that internal defects that might compete as sinks are manifestly lacking. Note that interstitials cannot possibly have sinks that are more distant than the external surface identified here as the sink for vacancies, and that their trajectories from creation to annihilation can therefore contribute no more than those of vacancies to the net diffusion (see the Appendix). Therefore the conclusion that at ≈ 700 K the front surface acts as the dominant vacancy sink seems quite firm.

A second conclusion pertains to irradiation effects. The plot of D_{RED} in Fig. 2 shows that the extra diffusion caused by the radiation field decreases systematically with decreasing temperature, first abruptly at the ordering transition, and then progressively further as the temperature is decreased in the ordered state. But the defect *production* by irradiation is essentially temperature-independent. Furthermore, in the steady state, all defects necessarily pass through a complete

life cycle from creation to annihilation; the magnitude of the enhanced diffusion simply reflects the creation rate and length of random walk each of the defects created per second defect undergoes in this life cycle. Therefore the observed reduction of the enhanced diffusion can only mean that the total diffusion *per defect* decreases as the temperature is lowered. Above we deduce that the kinetics just above T_c are first order, with the preponderance of interstitials annealing to fixed sinks near 700 K and with thermal vacancies at higher temperatures. Obviously this cannot remain true of the reduced D_{RED} at lower T. Provided that the free surface remains the dominant fixed sink, and the length of random walk it requires is not changed, we are thus drawn to conclude that recombination of vacancies with interstitials must, as T is lowered, overtake the drainage of defects to the front surface sink and becomes the dominant limit on the diffusion path length. For example, the factor 5 decrease of D_{RED} at T_c must mean that the defect kinetics below T_c for this level of irradiation enter the ''second order'' regime in which recombination dominates the defect life cycle.

We turn now to a quantitative discussion of radiation enhanced diffusion below T_c. The vacancy contribution $(c_v - \overline{c_v}) f_v D_v$ to the enhanced Cu diffusion may be written, according to the Appendix,

$$D = [(1+A)^{1/2} - 1] \frac{1+x}{2x} \overline{c}_v f_v D_v , \tag{6}$$

with

$$A = B \frac{4x}{(1+x)^2} \tag{6a}$$

in which

$$B = \frac{K_0 f_v}{\kappa_0^2 D_{\mathrm{Cu}}} . \tag{6b}$$

Here, we may write

$$x = K_{iv} \overline{c_i c_v} / K_{is} \overline{c_i} = \overline{c_v}(T) / \overline{c_v}(T_0) . \tag{6c}$$

In this equation T_0 is defined as the temperature at which recombination and flow to sinks are equally effective in annihilating a dilute population of interstitials. This form of x is convenient since the true vacancy concentration can only be guessed while its temperature dependence can be estimated reasonably reliably. Note that precisely the same binding and mobility factors enter into both the diffusion and the enhanced diffusion of Ni. It is therefore reasonable that the ratio of enhanced diffusion to diffusion for Ni is the same as that of Cu, so that the enhanced diffusion is obtained as

$$D_{\mathrm{Ni}}^{\mathrm{RED}} = [(1+A)^{1/2} - 1] \frac{1+x}{2x} D_{\mathrm{Ni}} . \tag{7}$$

This equation provides a basis on which experiment can be compared with prediction. Note that the vacancy contribution alone is calculated. Since the steady state condition requires that equal numbers of vacancies and interstitials diffuse to the front surface, however, interstitials must contribute a similar factor which differs only in the different correlation factors with which vacancies and interstitials induce atomic transport. Given an interstitialcy mechanism with correlation factor 0.422 the diffusion is expected to be larger by a factor of about 1.4.

Comparison of the observed RED for Ni with the calculated behavior over the range for which diffusion data are available is illustrated in Fig. 2. For this purpose only D_{Ni} and the constant B are needed, with D_{Cu} obtained from D_{Ni} as in Sec. IV A, and with the values of K_0 and κ_0^2 as given above. Predictions are shown for the two cases in which the crossover occurs at $T_0 = 670$ K, just above the transition, and $T_0 = 730$ K, well above the transition. The results do not depend strongly on the crossover temperature, and are generally within a factor 2 of the observed values. In particular, the weak temperature dependence is echoed in the predictions. The semiquantitative agreement is achieved without fitting parameters other than T_0, to which the results are evidently quite insensitive.

With regard to the temperature dependence of D_{RED} we note that, in the second order regime, the overall temperature dependence of host Cu follows the square root of the mobility of the less mobile defect, in this case the vacancy. Since jumping of Ni atoms requires slightly higher activation, the temperature dependence becomes somewhat more complex. Given the estimate in Eq. (6) of 1.05 eV for the vacancy formation energy, and the activation energies of 2.15 eV and 1.9 eV for Ni and Cu diffusion, respectively, from Fig. 1, one expects an activation energy of $\approx$0.65 eV. For comparison, the activation energy for D_{RED} of Ni below T_c is obtained from Fig. 2 as about 0.4 eV. For Pd RED the apparent activation energy is 0.7 eV which is to be compared with half the hopping energy, which gives 0.95 eV. While not identical, the two sets of measured and calculated values are sufficiently close for the explanation to remain reasonable, given the experimental complexities. Specifically, the very weak temperature dependence of the Ni RED, and the observed difference between Pd and Ni RED, are both reproduced satisfactorily without use of fitting parameters. Closer agreement is further inhibited by the variation of order parameter with temperature, which has not been included in this model. We comment on this point presently.

A marked failure of the predictions is that the calculations do not reproduce the large decrease of D_{RED} as the alloy orders at T_c. On both sublattices the observed enhanced diffusion is decreased by a factor 5, while the prediction decreases along with the thermal diffusion only by a factor closer to 2. This is a matter of great interest because the calculations are insensitive to free variables, and any phenomenon that affects D must equally affect D_{RED}. It is an important point that the reverse is *not* true, because the irradiated material contains heterogeneities associated with damage that have no counterpart in the unirradiated material. Therefore phenomena that change D_{RED} may nevertheless leave D unchanged. An explanation for the larger discontinuity in D_{RED} at T_c could be that the influence of heterogeneities induced by irradiation differs in the ordered and disordered materials. An example is the observation by Lang *et al.*[19] that point defects trap in the disorder surrounding a damage event in the otherwise ordered alloy. In unpublished research they show that the defect lingers until the damage is partially healed before escaping to reach a fixed sink. This behavior is not totally unexpected since the vacancy forma-

tion energy increases with chemical order in Cu_3Au. In this case the kinetics of the defect can no longer be predicted from the thermal diffusion and the sink geometry alone, and the radiation enhancement is changed. It seems possible that future studies of transient behavior will provide much added information about equilibrium under irradiation.

V. SUMMARY

In this paper we have shown that thermal and radiation enhanced diffusion in intermetallic compounds can be studied successfully using thin metal films grown by molecular beam epitaxy. As in earlier research on semiconductors, the time evolution of tracer profiles from buried layers can be examined *post facto* by secondary ion mass spectrometry for different annealing temperatures, and the diffusion deduced from the spread of the tracer. In the present case of Cu_3Au this works well both for thermal diffusion and for diffusion enhanced by an irradiation field, in this case provided by an ion beam. A fortunate feature of the present research is that irradiation levels below those that heat the sample or induce blistering are sufficient for radiation induced defects to attain concentrations comparable with those for thermal equilibrium, even above the ordering temperature. This can only be expected more generally for sufficiently low ordering temperatures.

The thermal diffusion determined here for temperatures above the ordering temperature T_c fits quite well with earlier results for higher temperatures, so that a consistent picture is now available for the entire range from T_c to T_m. This agreement requires that our results for Ni and Pd tracers be corrected for impurity-vacancy interactions by a factor ~ 30 that is consistent with actual observations for the diffusion of these elements in pure Cu and Au. We find an abrupt decrease in thermal diffusion at T_c that amount to factors of 2 and 4 on the Cu and Au sublattices, respectively. The difference is related in part to the geometrical fact that the Au sublattice lacks diffusion pathways that are confined to first neighbor jumps between Au sites. Au diffusion is therefore suppressed more than Ni below T_c by the need for antistructure configurations in diffusion pathways. This impediment causes a progressive depression of mobility as the temperature is decreased in the ordered phase. Some part of the reductions may arise from increased trapping of migrating defects at antistructure.

An important feature of this work is the experimental inference from measurements in a radiation field that the front surface of the sample is the dominant sink for vacancies. This has afforded a clear understanding of the kinetic regimes under which the experiments with He irradiation have been conducted. Under the experimental conditions there is a transition from marginally first order kinetics above the ordering temperature to increasingly second order kinetics at temperatures below T_c. There follows from this basis a semiquantitative description of the decrease of irradiation enhanced diffusion that take place as the temperature is reduced.

An exception to this general understanding is the decrease of D_{RED} at the ordering temperature itself, which for He irradiation exceeds the observed factor 2 reduction of thermal diffusion by a further factor of 2. This points to mechanisms that exist in the irradiated material that are both absent from the equilibrium alloy and, moreover, differ between the ordered and disordered phases. One possible example is the trapping of defects in disordered regions near a damage event in the ordered alloy.

ACKNOWLEDGMENTS

This research was supported in part by the Department of Energy, Basic Energy Sciences under Grant No. DEFG02-91ER45439. Use of facilities supported by the Materials Research Laboratory is gratefully acknowledged.

APPENDIX: DEFECT EQUILIBRIUM IN AN IRRADIATED THIN FILM

Here we formulate an accurate description of reaction kinetics that is explicitly adapted to the present interest in thin film systems. The discussion is based on a body of earlier work.[20] In what follows we first set up the kinetic mean field equations for spatially uniform defect populations in an explicit form, and then obtain expressions that describe steady state configurations.

In the present case, the dominant sink for freely migrating defects is believed to be the front surface of the film at $z=L$. For a uniform distribution of defects created by the radiation field the eigenfunctions of the diffusion equation, when the front surface alone acts as a sink, are $c_n(z,t)=C_n\exp(-t/\tau)\cos(2n+1)\pi z/2L$, with the $n=0,1,2,\ldots$ positive integers, and with eigenvalues $\tau_n^{-1}=[(2n+1)\pi/2L]^2D$. The D are defect diffusion coefficients. From explicit coefficients C_n it is found that fractions $8/\pi^2(2n+1)^2$ of the total defect production fall into different terms, n. It will suffice for the present purposes to consider only the first term, with

$$dc_0/dt=-(\pi/2L)^2Dc_0, \tag{A1}$$

and which contains $\approx 80\%$ of the production, recognizing that the remaining fraction starts closer to the sink and annihilate somewhat faster.

In addition to the sink terms it is necessary to represent recombination. Assume that the faster moving defects, specifically interstitials, move with diffusion coefficient D through a random distribution of opposite defects (vacancies) located at fixed sites with uniform fractional concentration c_i. The interstitial undergoes uncorrelated jumps w times each second with a jump distance l, so its mean square displacement is $\langle R^2\rangle=6Dt=wl^2$, and therefore $D=wl^2/6$. This random walk achieves wt steps in time t, and permits the vacancy to inspect a number $wtl\cdot\pi\rho^2/\Omega=6Dt\cdot\pi\rho^2/l\Omega$ of sites for possible recombination with interstitials. Here Ω is the atomic volume and ρ is the radius of the tube inside which interstitials recombine with vacancies. Upon including an analogous term because vacancies also jump we find that the concentration decays by recombination as

$$\frac{dc_v}{dt}=\frac{dc_i}{dt}=-\frac{\lambda_vD_v+\lambda_iD_i}{a^2}c_vc_i, \tag{A2}$$

in which a is the lattice parameter and the λ are geometrical factors. Specifically for the vacancy $l=a/\sqrt{2}$, $\Omega=a^3/4$, and as the recombination distance ρ is not known we write it $\rho=\varepsilon a$, as a multiple ε of the lattice parameter a, in the expectation that $\varepsilon\sim 1$. A further term arises from the self-intersecting character of the random walk which reduces the recombination efficiency in two ways. First, the short-range character of random walks causes the volume factor $wt\cdot l\pi\rho^2$ to be an overestimate by a factor that depends on the ratio ρ/l. An immediate return jump, for example, eliminates two successive jumps and this happens one twelfth of the time; successive jumps in directions that differ by more than 90° likewise are less effective, and this occurs four of twelve times. In addition to short range terms of this type, it sometimes happens that the random walk intersects itself after numerous intervening jumps, and these cause further reductions of the predicted recombination. Without detailed accounting we estimate that these several contributions reduce the values of the λ by about a factor 2 to leave finally

$$\lambda_v\sim 12\sqrt{2}\,\pi\varepsilon^2=53.3\varepsilon^2. \tag{A3}$$

This analysis yields a value very similar to that suggested by Damask and Dienes.[21] The detailed structure of the constants λ_j does not affect the interpretation of the present results.

We can now write down the mean-field equations for homogeneous reaction among concentrations c_v, c_i, of vacancies and interstitials which are being produced by irradiation at a rate K_0 per site. They are

$$\frac{dc_v}{dt}=K_0-K_{iv}c_ic_v-K_{vs}(c_v-\overline{c_v})+K_{iv}\overline{c_ic_v}, \tag{A4}$$

$$\frac{dc_i}{dt}=K_0-K_{iv}c_ic_v-K_{is}(c_i-\overline{c_i})+K_{iv}\overline{c_ic_v}. \tag{A5}$$

Here,

$$K_{iv}=\frac{\lambda_vD_v+\lambda_iD_i}{a^2}, \tag{A6}$$

$$K_{vs}=(\pi/2L)^2D_v, \quad K_{is}=(\pi/2L)^2D_i. \tag{A7}$$

In these equations the terms involving the equilibrium concentrations $\overline{c_v}, \overline{c_i}$, are introduced to ensure that these same defect levels are indeed the steady state solutions in the absence of radiation when $K_0=0$.

The steady state solution, obtained by subtraction after setting the time derivatives to zero is

$$K_{vs}(c_v-\overline{c_v})=K_{is}(c_i-\overline{c_i}), \tag{A8}$$

which when used to eliminate c_i gives

$$\frac{K_{iv}K_{vs}}{K'_{vs}K_{is}}(c_v-\overline{c_v})^2+(c_v-\overline{c_v})-\frac{K_0}{K'_{vs}}=0, \tag{A9}$$

in which

$$K'_{vs}=K_{vs}+K_{iv}\overline{c_i}+\frac{K_{iv}K_{vs}}{K_{is}}\overline{c_v}. \tag{A10}$$

Note that these equations describe the *excess* vacancy concentration over and above the equilibrium level. An analogous equation for interstitials is obtained by substitution for $(c_v-\overline{c_v})$ in terms of $(c_i-\overline{c_i})$, using the relationship (A8) for the steady state given above. When the equilibrium levels are zero the same relationships hold but with K'_{vs} and K'_{is} reducing to K_{vs} and K_{is}, as made apparent by Eq. (A10).

Equation (A9) is easily solved to yield the irradiation-induced populations

$$\begin{aligned}c_v-\overline{c_v}&=[(1+A)^{1/2}-1](K'_{vs}K_{is}/2K_{iv}K_{vs})\\&=(c_i-\overline{c_i})K_{is}/K_{vs},\end{aligned} \tag{A11}$$

with

$$A=\frac{4K_{iv}K_{vs}K_0}{(K'_{vs})^2K_{is}}. \tag{A12}$$

This reduces for $A\ll 1$ (first order kinetics) to

$$c_v-\overline{c_v}=K_0/K'_{vs}, \quad c_i-\overline{c_i}=K_0/K'_{is}, \tag{A13}$$

and for $A\gg 1$ (second order kinetics) to

$$c_v-\overline{c_v}=\left(\frac{K_0K_{is}}{K_{iv}K_{vs}}\right)^{1/2}, \quad c_i-\overline{c_i}=\left(\frac{K_0K_{vs}}{K_{iv}K_{is}}\right)^{1/2}. \tag{A14}$$

It is frequently important to identify the transition from first order to second order behavior, which occurs when the first term in Eq. (A9) exceeds the second term:

$$\frac{K_{iv}K_{vs}}{K'_{vs}K_{is}}(c_v-\overline{c_v})>1. \tag{A15}$$

In comparing the second and third terms for K'_{vs} in Eq. (A10), that for the dominant defect is always the larger, in the present case of dominant vacancy disorder the last term, giving

$$K'_{vs}=K_{vs}(1+K_{iv}\overline{c_v}/K_{is}). \tag{A16}$$

The condition for the transition to second order may now be written

$$\frac{x}{1+x}\,\frac{c_v-\overline{c_v}}{\overline{c_v}}>1, \tag{A17}$$

with

$$x=K_{iv}\overline{c_ic_v}/K_{is}\overline{c_i}. \tag{A18}$$

In Eq. (A18), the numerator is the rate at which interstitials recombine with vacancies and the denominator is the rate at which they reach sinks, both evaluated *for thermal equilibrium*. Thus when vacancies are so plentiful in equilibrium that they trap interstitials more effectively than the sinks can $(x>1)$, the transition then occurs when irradiation increases the vacancy population by a factor ~ 2. When, on the other hand, the sinks provide the more effective drain on the interstitial concentration, then $x<1$, and the vacancy population must be increased by a factor $\sim x^{-1}$ before the vacancies can annihilate more interstitials than do fixed sinks, and the transition to second order kinetics occurs. In the calculations of

Sec. IV, all details of the rate constants K_{ij} cancel other than the ''crossover temperature'' T_0 at which $x=1$.

The additional radiation-induced diffusion in excess of the equilibrium contribution, viz.

$$D=\overline{c_v}f_vD_v+\overline{c_i}f_iD_i\,, \tag{A19}$$

is

$$D_{\mathrm{RED}}=(c_v-\overline{c_v})f_vD_v+(c_i-\overline{c_i})f_iD_i\,. \tag{A20}$$

Here, f_v and f_i are correlation factors that relate the defect diffusion to the resulting atomic diffusion. The general form is obtained by insertion of Eq. (A11) in Eq. (A20). For the two limits of small and large A specified in Eqs. (A13) and (A14) the results are

$$D_{\mathrm{RED}}=K_0\left(\frac{f_vD_v}{K'_{vs}}+\frac{f_iD_i}{K'_{is}}\right)\quad(\text{first order kinetics}) \tag{A21}$$

and

$$D_{\mathrm{RED}}=f_vD_v\left(\frac{K_{iv}K_{is}}{K_0K_{vs}}\right)^{1/2}+f_iD_i\left(\frac{K_{iv}K_{vs}}{K_0K_{is}}\right)^{1/2}\quad(\text{second order kinetics}). \tag{A22}$$

In both cases the two defect species contribute equally to the diffusion, given equal correlation factors, provided that their sinks are equally effective. This is made evident by the fact the sink efficiencies contain the diffusion coefficients, and the cancellation makes the two terms depend identically on $D_v\,,D_i\,.$

[1] R. S. Averback and T. Diaz de la Rubia, in *Solid State Physics*, edited by H. Ehrenreich and F. Spaepen (Academic Press, New York, 1998), Vol. 51, p. 281.

[2] See, e.g., T. H. Blewitt and R. R. Coltman, Acta Metall. **2**, 549 (1954).

[3] Y. S. Lee, R. S. Averback, and C. P. Flynn, Philos. Mag. Lett. **70**, 269 (1994).

[4] See, for details, J. F. Ziegler, J. Biersack, and U. Littmark, *The Stopping and Range of Ions in Matter* (Pergamon, New York, 1985).

[5] S. Benci, G. Gasparrini, E. Germagnoli, and G. Schianchi, J. Phys. Chem. Solids **26**, 687 (1965).

[6] T. Hashimoto and K. Yamamoto, Philos. Mag. A **69**, 11 (1994).

[7] D. Lazarus, Phys. Rev. **93**, 973 (1954); A. D. LeClaire, Philos. Mag. **7**, 141 (1962).

[8] See, e.g., H. Mehrer, in *Diffusion in Metal*, Landolt Börnstein, New Series, Vol. 28 (Springer-Verlag, Berlin, 1991), and references therein.

[9] T. Ito, S. Ishioka, and M. Koiwa, Philos. Mag. A **62**, 499 (1990).

[10] H. B. Huntington (private communication).

[11] E. W. Elcock and C. W. McCombie, Phys. Rev. **109**, 606 (1958).

[12] E. W. Elcock, Proc. Phys. Soc. London **73**, 250 (1959).

[13] R. Kikuchi and H. Sato, J. Chem. Phys. **57**, 4962 (1972).

[14] J. M. Cowley, Phys. Rev. **77**, 669 (1950).

[15] Y. S. Lee, Ph.D. dissertation, University of Illinois at Urbana-Champaign, 1996.

[16] R. A. Vargas, M. B. Salamon, and C. P. Flynn, Phys. Rev. B **17**, 269 (1977).

[17] D. J. Bacon, in *Computer Simulation in Materials Science*, edited by H. Kirchner, L. Kubin, and V. Pontikis (Kluwer Academic Publishers, Dordrecht, 1996), p. 189.

[18] R. S. Averback, R. Benedek, and K. L. Merkle, Phys. Rev. B **18**, 4156 (1978).

[19] E. Lang, L. Wei, R. S. Averback, and C. P. Flynn (unpublished).

[20] See, e.g., and references therein, R. Sizmann, J. Nucl. Mater. **69/70**, 386 (1978).

[21] A. C. Damask and G. J. Dienes, in *Studies in Radiation Effects*, edited by G. J. Dienes (Gordon and Breach, New York, 1967), Vol. 2.